Edelweiss Applied Science and Technology
ISSN: 2576-8484
Vol. 10, No. 9, 290-304
2026
Publisher: Learning Gate
DOI: 10.55214/2576-8484.v10i9.13602

Robust NMPC–EKF framework for stabilization of an inverted pendulum on a cart under disturbances and model uncertainties

Labane Chrif[1*], Merah Abdelkader[2], Mekkaoui Mohammed[3]
[1,2,3]University of Saida Dr Moulay Tahar, Faculty of Sciences and Technology, Department of Electrotechnics and Automation, Saida, Algeria; chrif.labane@univ-saida.dz (L.C) merah.abdelkader@univ-saida.dz (M.A.) mekkaoui.mohammed@univ-saida.dz (M.M).
[1,3]Laboratory of Physico-Chemical Studies, 20 000, 12 Laboratory Electrotechnics Engineering, Algeria.

Abstract: The inverted pendulum on a cart is a nonlinear and inherently unstable benchmark system widely used to evaluate advanced control strategies. This paper presents a Nonlinear Model Predictive Control (NMPC) approach for stabilizing and regulating the position of an inverted pendulum–cart system in the presence of external disturbances and model uncertainties. The nonlinear dynamics are derived using the Euler–Lagrange formulation and discretized for predictive-control implementation. An Extended Kalman Filter (EKF) is employed to estimate the unmeasured velocity states from available position and angle measurements. At each sampling instant, the NMPC controller solves a constrained finite-horizon optimization problem using a Sequential Quadratic Programming (SQP) algorithm while explicitly considering state and input constraints. To highlight the benefits of nonlinear prediction, the proposed controller is compared with a conventional Linear Quadratic Regulator (LQR) under moderately and severely nonlinear benchmark scenarios. Simulation results show that both controllers provide satisfactory performance under moderately nonlinear operating conditions. However, under severe nonlinearities, disturbances, and parameter uncertainties, the LQR controller loses stability, whereas the Nonlinear MPC controller successfully maintains pendulum stabilization and cart-position regulation. The obtained results demonstrate the superior robustness, disturbance-rejection capability, and wider operating range of the proposed Nonlinear MPC strategy, confirming its suitability for controlling nonlinear and unstable dynamical systems.
Keywords: *Inverted pendulum cart system, Nonlinear MPC, Nonlinear system dynamics, Uncertainty, Disturbance.*

1. Introduction

The inverted pendulum system is one of the most widely studied benchmark problems in control engineering because of its nonlinear, unstable, and underactuated dynamics. Without appropriate control action, the pendulum naturally falls from its upright equilibrium position. Therefore, a control force must be applied to the cart to continuously balance the pendulum while simultaneously regulating the cart's motion. Owing to these challenging characteristics, the inverted pendulum has become a standard platform for the development and validation of advanced control strategies [1].

Beyond its theoretical significance, the inverted pendulum model is representative of several practical engineering systems. Examples include rocket attitude stabilization during launch, self-balancing personal transportation devices such as the Segway, humanoid robots during walking, and various robotic balancing systems. Consequently, the inverted pendulum remains an important benchmark for evaluating the performance and robustness of modern control algorithms.

Several configurations of inverted pendulum systems have been investigated in the literature, including cart inverted pendulums, rotary inverted pendulums, mobile inverted pendulums, and related nonlinear balancing systems [1, 2]. Among these configurations, the cart inverted pendulum has been

History: Received: 22 June 2026; Revised: 25 August 2026; Accepted: 28 August 2026; Published: 17 September 2026
* Correspondence: chrif.labane@univ-saida.dz

extensively employed for more than seven decades as a benchmark control problem because of its relatively simple structure and highly nonlinear behavior [3]. The main control objectives generally involve swing-up control, stabilization around the unstable upright equilibrium, and cart-position tracking [2, 4].

Numerous control approaches have been proposed for inverted pendulum systems, including proportional–integral–derivative (PID) [5] control, state-feedback control, optimal control [6], robust control, adaptive control, and model predictive control (MPC) [7-9]. Among these techniques, model predictive control has attracted considerable attention because it explicitly incorporates system constraints while optimizing future control actions over a finite prediction horizon [4]. This capability enables improved tracking performance and systematic handling of actuator and state limitations [8].

For nonlinear systems such as the inverted pendulum, Nonlinear Model Predictive Control (NMPC) provides additional advantages by directly exploiting the nonlinear plant dynamics without relying on local linear approximations. As a result, NMPC can achieve improved performance over a wider operating range, particularly in the presence of disturbances and nonlinear effects. However, the practical implementation of NMPC remains challenging because a constrained nonlinear optimization problem must be solved online at every sampling instant. Consequently, computational complexity and real-time feasibility remain important research issues in NMPC applications [10-12].

Several studies have investigated the application of NMPC to inverted pendulum systems. Previous works have demonstrated the effectiveness of NMPC for stabilization and trajectory-tracking tasks while satisfying operational constraints [2, 8]. Nevertheless, many existing studies focus primarily on nominal operating conditions and provide limited analyses of controller performance under significant nonlinearities, disturbances, and model uncertainties. Furthermore, comparative assessments of nonlinear predictive controllers and conventional linear control strategies remain relatively limited, particularly when the system operates far from its equilibrium region.

Motivated by these observations, this paper investigates the application of an NMPC strategy for the stabilization and regulation of an inverted pendulum mounted on a cart under external disturbances and parameter uncertainties. The nonlinear dynamics of the system are modeled using the Euler–Lagrange formulation, while an Extended Kalman Filter (EKF) is employed to estimate the unmeasured states required by the predictive controller. The NMPC optimization problem is solved online using a Sequential Quadratic Programming (SQP) algorithm. To highlight the benefits of nonlinear prediction, the proposed controller is compared with a conventional Linear Quadratic Regulator (LQR) under moderately and severely nonlinear benchmark scenarios. The effectiveness of the proposed approach is evaluated through reference-tracking and disturbance-rejection simulations, and quantitative performance indicators are reported to assess the closed-loop behavior.

The remainder of this paper is organized as follows. Section 2 presents the mathematical modeling of the inverted pendulum system. Section 3 describes the design of the NMPC controller and the EKF-based state-estimation scheme. Section 4 discusses the simulation results and comparative performance evaluation of the LQR and NMPC controllers under different nonlinear operating conditions. Finally, Section 5 summarizes the main conclusions and outlines future research directions.

.

2. Mathematical Modelling of the Inverted Pendulum on a Cart A

The inverted pendulum on a cart is one of the most widely used benchmark systems in nonlinear control because of its inherently unstable and underactuated nature [1, 2]. The system consists of a cart of mass M moving along a horizontal track and a pendulum of mass m attached to the cart by a rigid rod of length l, as illustrated in Figure 1. A control force u is applied to the cart to regulate its position while maintaining the pendulum in the unstable upright equilibrium position. Owing to the strong coupling between the cart's translational motion and the pendulum's rotational motion, the resulting dynamics are highly nonlinear and present significant control challenges.

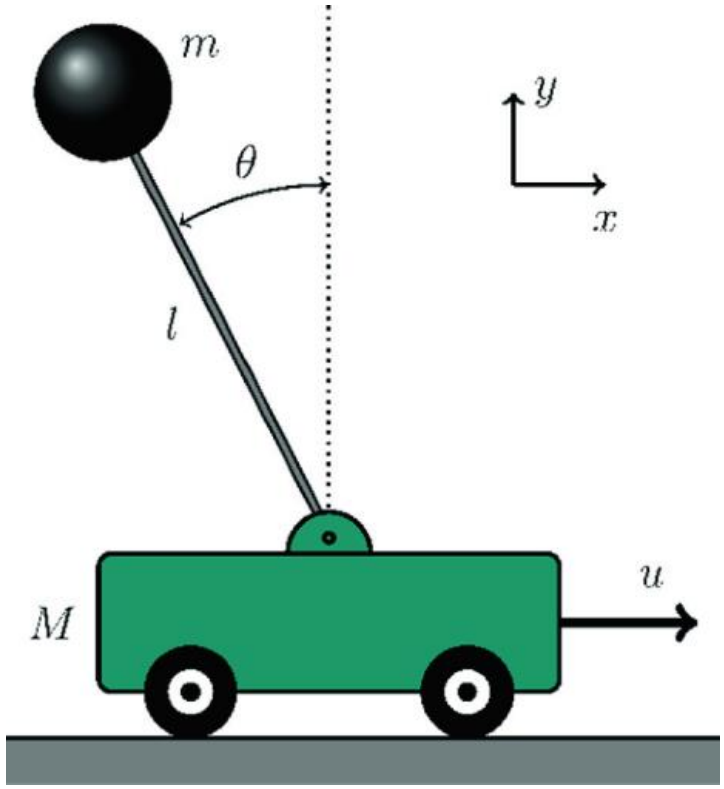

Figure 1.
Modelling of an Inverted Pendulum on Cart.

To obtain a realistic description of the system, viscous friction acting on the cart is taken into account through a damping coefficient b. The pendulum rod is assumed to be rigid and massless, while the pendulum mass is concentrated at its center of gravity. The generalized coordinates are selected as the cart position p and the pendulum angular displacement θ, measured with respect to the upright vertical position.

Using the Euler–Lagrange formulation, the nonlinear equations of motion can be derived by considering the kinetic and potential energies of the cart–pendulum assembly. The resulting model describes the coupled translational and rotational dynamics under the action of the control force and external disturbances [1, 13]. To evaluate the disturbance-rejection capability of the proposed controller, an external disturbance $d(t)$ is introduced into the cart dynamics [14, 15].
For controller design and state prediction, the system is represented by the state vector

$$X = [p \quad \dot{p} \quad \theta \quad \dot{\theta}]^T \tag{1}$$

where $p$and $\dot{p}$ denote the cart's position and velocity, respectively, while $\theta$and $\dot{\theta}$ represent the pendulum's angular displacement and angular velocity. Based on this state representation, the nonlinear state-space model is expressed as:

$$\dot{p} = \dot{p}$$

$$\dot{\theta} = \dot{\theta} \tag{2}$$

$$\ddot{p} = \frac{u + d(t) - b\dot{p} + ml\dot{\theta}^2 \sin\theta + mg\sin\theta\cos\theta}{M + m - m\cos^2\theta}$$

$$\ddot{\theta} = \frac{(u + d(t))\cos\,\theta - b\dot{p}\cos\,\theta - ml\dot{\theta}^2\sin\,\theta\cos\,\theta + (M + m)g\sin\,\theta}{l(M + m - m\cos^2\theta)}$$

The nonlinear dynamics can be compactly written as [16]

$$\dot{X} = f(X, u, d) \tag{3}$$

where $f(\cdot)$ denotes the nonlinear state-transition function employed by the predictive controller.
The measured output vector is selected as [1, 16-18]

$$Y = \begin{bmatrix} p \\ \theta \end{bmatrix} \tag{4}$$

which corresponds to the cart position and pendulum angle available for feedback. These variables sufficiently characterize the system behavior and constitute the primary control objectives.

The control problem addressed in this work consists of simultaneously stabilizing the pendulum around the unstable upright equilibrium position and driving the cart toward a desired reference position p_r. Consequently, the controller must ensure that the pendulum angle converges to zero while the cart accurately tracks the prescribed reference trajectory. In addition, satisfactory performance must be maintained in the presence of external disturbances and actuator limitations.

Unlike linearized models, which are valid only within a narrow neighborhood of the equilibrium point, the nonlinear formulation adopted in this study preserves the complete dynamics of the pendulum–cart system. This representation enables the predictive controller to accurately capture the plant's nonlinear behavior over a wider operating range, thereby improving stabilization, tracking accuracy, and disturbance-rejection performance. The resulting nonlinear model serves as the foundation for the NMPC design developed in the following section.

2.1. Linear Quadratic Regulator Controller

Modern control theory has made a significant impact on the aircraft industry in recent years [16, 17]. LQR is a method in modern control theory that uses a state-space approach to analyze such a system. Using state-space methods, it is relatively simple to work with a multi-output system. The system can be stabilized using a full-state feedback system. The configuration of this control system is shown in the simulation results.

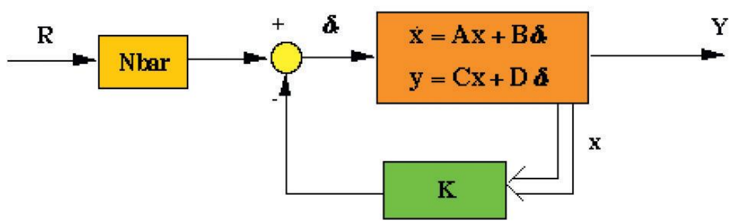

Figure 2.
Full-state feedback controller with reference input.

In designing an LQR controller, the *lqr* function in Matlab can be used to determine the value of the vector K which determines the feedback control law. This is done by choosing two parameter values, the input $R = 1$ and $Q = C^T * C$ Where C^T is the matrix transpose of C. The controller can be tuned by changing the nonzero elements in the Q matrix, which is done in the m-file code shown below [17].

$R = 1$

$Q = [0000, 0000, 0000, 000x]$

$K = lqr[A, B, Q, R]$

Edelweiss Applied Science and Technology
ISSN: 2576-8484
Vol. 10, No. 9: 290-304, 2026
DOI: 10.55214/2576-8484.v10i9.13602

Consequently, by tuning the value of $x = 500$, the following values of matrix K are obtained. If x is increased further, the response should improve even more. However, for this case, the value of $x = 500$ is chosen because it satisfies the design requirements while keeping x as small as possible.

To reduce the steady-state error of the system output, a constant gain, *Nbar*, should be added after the reference. With a full-state feedback controller, all the states are fed back. The steady-state values of the states should be computed, multiplied by the selected gain K, and used as a new reference for computing the input. *Nbar* can be found using a user-defined function in an M-file. The method used in the simulation involves exporting both the value of matrix K and the constant gain. For this controller design, the value of the constant gain *Nbar* are found to be, $Nbar = 100$ [15, 17].

3. Nonlinear Model Predictive Control Design

Nonlinear Model Predictive Control (NMPC) is adopted to stabilize the inverted pendulum around its unstable upright equilibrium position while simultaneously ensuring accurate cart-position tracking in the presence of external disturbances. Unlike conventional linear control techniques, NMPC directly exploits the nonlinear dynamics of the plant and explicitly incorporates system constraints into the control design. This capability makes NMPC particularly suitable for highly nonlinear and unstable systems such as the inverted pendulum on a cart.

The overall closed-loop NMPC–EKF control architecture is illustrated in Figure 2. The framework integrates an NMPC controller, a nonlinear inverted pendulum–cart plant, sensor measurements, and an Extended Kalman Filter (EKF). The EKF reconstructs the complete state vector required by the NMPC, which computes the optimal control force and applies it to the plant in a receding-horizon manner.

At each sampling instant, the controller predicts the future evolution of the nonlinear system over a finite prediction horizon using the nonlinear model developed in Section 2. An optimal sequence of control inputs is then computed by solving a constrained optimization problem. Following the receding-horizon principle, only the first element of the optimal control sequence is applied to the plant, while the optimization procedure is repeated at the next sampling instant using updated state information.

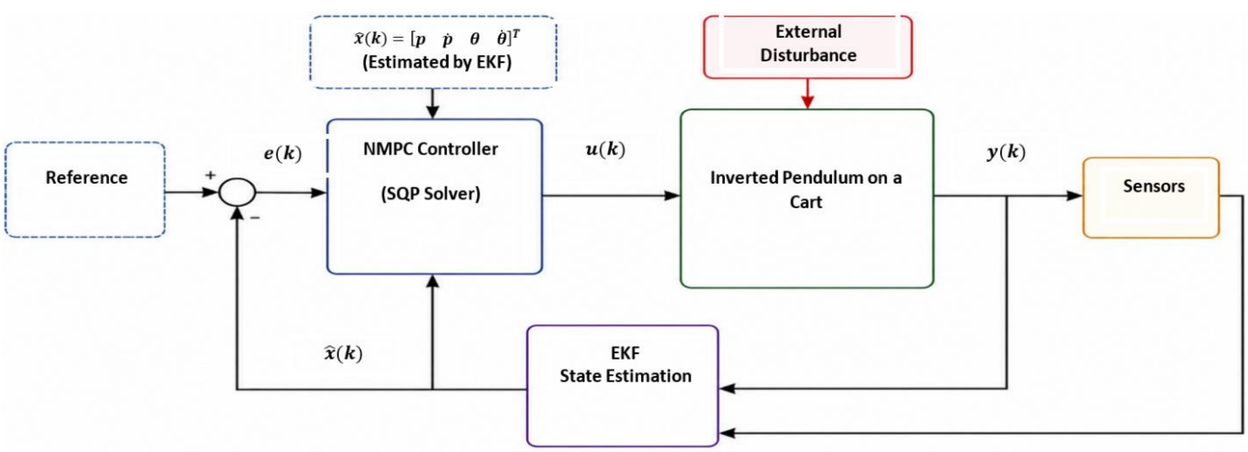

Figure 3.
Closed-loop architecture of the proposed NMPC–EKF control system for the inverted pendulum on a cart.

3.1. Prediction Model

The nonlinear state-space model derived in Section 2 is employed as the prediction model for the NMPC controller. After discretization with a sampling period T_s, the system can be represented as Bacha, et al. [19]

$$X_{k+1} = f_d(X_k, u_k) \tag{5}$$

where X_k denotes the state vector at the sampling instant k, u_k is the control input applied to the cart, and $f_d(\cdot)$ represents the discrete-time nonlinear dynamics.

Starting from the current state estimate X_k, the future system behavior is predicted over a prediction horizon $N_p$according to Fahmizal, et al. [11]

$$X_{k+i+1} = f_d(X_{k+i}, u_{k+i}), i = 0, \ldots, N_p - 1 \tag{6}$$

The resulting predicted state trajectory is subsequently used by the optimization algorithm to determine optimal control actions.

3.2. NMPC Optimization Problem

The control objective is formulated as a finite-horizon optimal control problem. The cost function is defined as in Chrif and Zemalache Meguenni Kadda [2]

$$J = \sum_{i=0}^{N_p-1} [(X_{k+i} - X_r)^T Q (X_{k+i} - X_r) + u_{k+i}^T R u_{k+i} + \Delta u_{k+i}^T R_{\Delta u} \Delta u_{k+i}] + (X_{k+N_p} - X_r)^T P (X_{k+N_p} - X_r) \tag{7}$$

where Q, R, and P are positive semidefinite weighting matrices associated with state tracking, control effort, and terminal-state regulation, respectively [10]. The matrix $R_{\Delta u}$ penalizes excessive variations in the control input and contributes to smoother actuator commands.

The reference state vector is selected as

$$X_r = [p_r \quad 0 \quad 0 \quad 0]^T \tag{8}$$

where $p_r$denotes the desired cart position.

The optimal control sequence is obtained by minimizing the cost function subject to the nonlinear prediction model and operational constraints [7]

$$u_{\min} \leq u_k \leq u_{\max} \tag{9}$$

and

$$X_k \in \Omega$$

where Ω denotes the admissible state set. These constraints ensure physically feasible control actions while preserving closed-loop stability and safety.

3.3. Receding-Horizon Strategy

The NMPC controller operates according to the receding-horizon principle illustrated in Figure 3. At each sampling instant, the current state of the system is measured or estimated and used as the initial condition for predicting future states [11].

Edelweiss Applied Science and Technology
ISSN: 2576-8484
Vol. 10, No. 9: 290-304, 2026
DOI: 10.55214/2576-8484.v10i9.13602

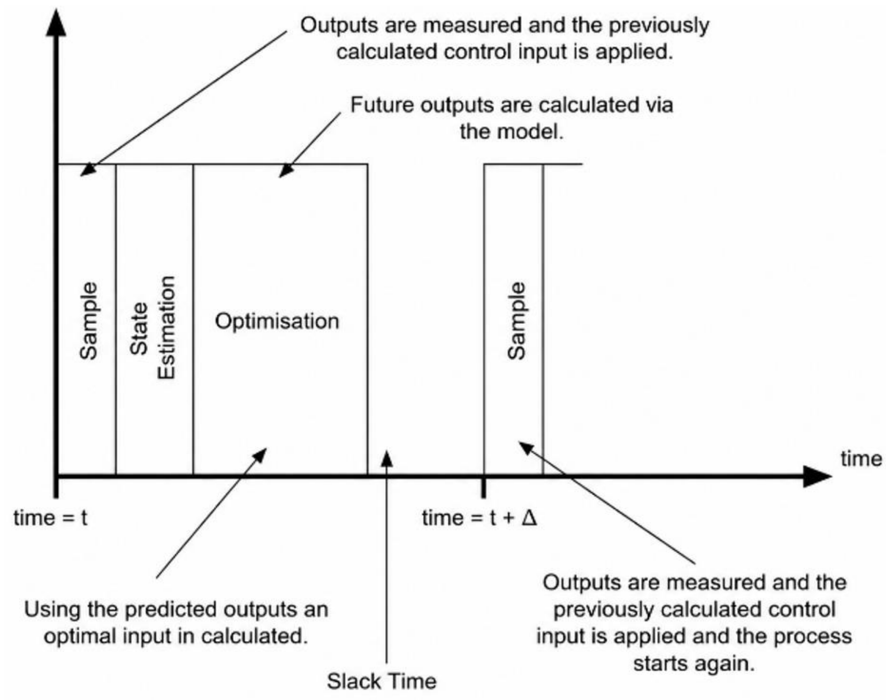

Figure 4.
Timing sequence of the receding-horizon NMPC strategy.

The optimization problem is solved over the prediction horizon, producing an optimal control sequence [1, 4]

$$U^* = \left[u_k^*, u_{k+1}^*, \dots, u_{k+N_p-1}^*\right] \tag{10}$$

Only the first control action is applied to the plant,

$$u(k) = u_k^* \tag{11}$$

while the remaining control moves are discarded.

At the next sampling instant, new measurements become available, the prediction horizon shifts forward, and a new optimization problem is solved. This continuous feedback mechanism enables the controller to compensate for disturbances, parameter variations, and modeling uncertainties while maintaining high tracking accuracy.

3.4. Extended Kalman Filter-Based State Estimation

Since the NMPC controller requires knowledge of the complete state vector

$$X = [p \quad \dot{p} \quad \theta \quad \dot{\theta}]^T \tag{12}$$

To perform state prediction and optimization, only the cart position p and pendulum angle θ are typically measured. Therefore, an Extended Kalman Filter (EKF) is employed to reconstruct the unmeasured velocity states $\dot{p}$ and $\dot{\theta}$ [6].

The nonlinear system is represented by

$$X_{k+1} = f_d(X_k, u_k) + w_k \tag{13}$$
$$Y_k = h(X_k) + v_k$$

where w_k and v_k denote zero-mean Gaussian process and measurement noises with covariance matrices Q_w and R_v, respectively.
The prediction stage is given by Bouzoualegh, et al. [8]

$$\hat{X}_{k|k-1} = f_d(\hat{X}_{k-1|k-1}, u_{k-1}) \tag{14}$$

$$P_{k|k-1} = A_k P_{k-1|k-1} A_k^T + Q_w$$

where

$$A_k = \frac{\partial f_d(X,u)}{\partial X} |_{\hat{X}_{k-1|k-1}}$$

is the Jacobian matrix of the nonlinear dynamics.
The innovation vector is computed as

$$r_k = Y_k - h(\hat{X}_{k|k-1}) \tag{15}$$

and the Kalman gain is obtained from Bouzoualegh, et al. [8]

$$K_k = P_{k|k-1} H_k^T \left(H_k P_{k|k-1} H_k^T + R_v\right)^{-1} \tag{16}$$

where

$$H_k = \frac{\partial h(X)}{\partial X} |_{\hat{X}_{k|k-1}}$$

is the measurement Jacobian matrix.
The corrected state estimate is then computed as Pete and Deosarkar [20] and Wei, et al. [21]

$$\hat{X}_{k|k} = \hat{X}_{k|k-1} + K_k r_k \tag{17}$$

with covariance update

$$P_{k|k} = (I - K_k H_k) P_{k|k-1} \tag{18}$$

The estimated state vector $\hat{X}_{k|k}$ is subsequently supplied to the NMPC controller and used as the initial condition for predicting future states [20].

3.5. Online Control Implementation

At each sampling instant, the NMPC optimization problem is solved online using a Sequential Quadratic Programming (SQP) algorithm. SQP is particularly suitable for constrained nonlinear optimization because it transforms the original nonlinear problem into a sequence of quadratic subproblems that can be solved efficiently [11, 12].
The online control procedure can be summarized as follows [22, 23]:

1. Measure cart position p and pendulum angle θ.
2. Estimate the complete state vector using the EKF.
3. Predict future system behavior over the prediction horizon.
4. Solve the constrained NMPC optimization problem using SQP.
5. Apply the first optimal control action to the cart.
6. Shift the prediction horizon forward and repeat the procedure at the next sampling instant.

The resulting NMPC framework combines nonlinear prediction, state estimation, and constrained optimization to achieve accurate tracking, effective pendulum stabilization, and robust disturbance rejection.

4. Results and Discussion

The performance of the proposed NMPC controller is evaluated and compared with that of the conventional LQR controller under two nonlinear benchmark scenarios of increasing difficulty. Both controllers are tested using the uncertain nonlinear plant model and identical disturbance conditions to ensure a fair comparison. The first scenario, referred to as the Moderately Nonlinear Benchmark, considers an initial pendulum deviation of $35°$ and a disturbance amplitude of 5 N. The second scenario, denoted as the Severely Nonlinear Benchmark, increases the initial angular deviation to $38°$ and the disturbance amplitude to 7 N, thereby intensifying the nonlinear effects and control challenge. The corresponding simulation conditions and uncertain model parameters are summarized in Tables 1 and 2 [24].

The NMPC controller employed a sampling period of $T_s = 0.05$s and a prediction horizon of $N_p = 15$. At each control update, the constrained optimization problem was solved online using SQP.

Table 1.
Benchmark scenarios used for LQR and NMPC performance evaluation.

Parameter	Moderately Nonlinear Benchmark	Severely Nonlinear Benchmark
Initial cart position $\boldsymbol{p(0)}$	0 m	0 m
Initial cart velocity $\dot{\boldsymbol{p}}\boldsymbol{(0)}$	0 m/s	0 m/s
Initial pendulum angle $\boldsymbol{\theta(0)}$	$35°$	$38°$
Initial angular velocity $\dot{\boldsymbol{\theta}}\boldsymbol{(0)}$	0 rad/s	0 rad/s
Control force limit	± 7N	± 7N
Disturbance amplitude	5 N	7 N
Disturbance start time	3.5 s	3.5 s
Disturbance end time	4.5 s	4.5 s
Plant model	Uncertain nonlinear model	Uncertain nonlinear model

Table 2.
Nominal and uncertain model parameters.

Parameter	Description	Nominal Model	Uncertain Model
$\boldsymbol{M}$	Cart mass (kg)	0.50	0.40
$\boldsymbol{m}$	Pendulum mass (kg)	0.30	0.40
$\boldsymbol{l}$	Pendulum length (m)	0.50	0.40
$\boldsymbol{b}$	Viscous friction coefficient (N·s/m)	0.10	0.05
$\boldsymbol{g}$	Gravitational acceleration (m/s^2)	9.81	9.81

The simulation results presented in the following subsections compare the transient response, stabilization capability, disturbance rejection, and control effort of both controllers under moderate and severe nonlinear operating conditions. This comparative analysis highlights the advantages and limitations of NMPC relative to the classical LQR approach when the system is subjected to significant nonlinearities, parameter uncertainties, and external disturbances.

.

4.1. Moderately Nonlinear Benchmark

Figures 5 and 6 show that both controllers exhibit similar cart-position and cart-velocity responses, although the NMPC controller produces a slightly smaller cart excursion and faster recovery following the disturbance. Likewise, the pendulum-angle and angular-velocity responses shown in Figures 7 and 8 remain well bounded for both controllers, with only minor differences during the transient phase. The control efforts depicted in Figure 9 are also comparable, indicating that the performance improvements achieved by NMPC are obtained without a significant increase in actuator demand.

The quantitative results reported in Table 3 confirm these observations. Compared with LQR, the NMPC controller reduces the maximum cart displacement by 12.08%, the RMS cart displacement by 4.40%, and the settling time by 14.34%. In addition, the tracking performance, measured by the

$ITAE_\theta$ index, is improved by 31.98%, indicating faster attenuation of the angular deviation. However, the RMS pendulum angle remains nearly identical for both controllers, with a slight advantage in favor of LQR (2.10%). Overall, the results indicate that, under moderately nonlinear operating conditions, both controllers provide satisfactory stabilization performance, while NMPC achieves modest improvements in transient response and disturbance rejection.

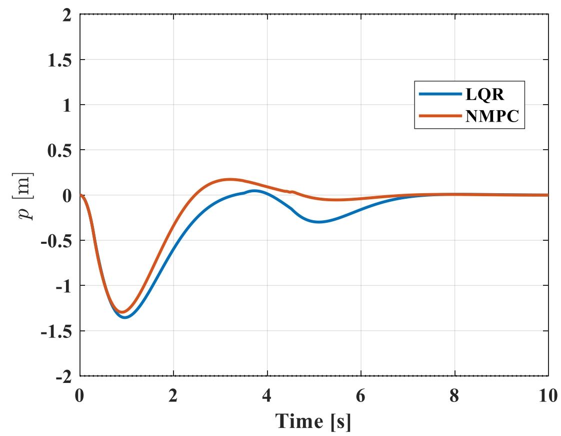

Figure 5.
Cart position.

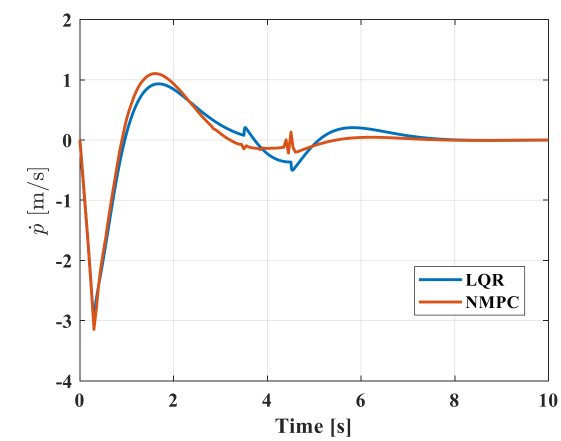

Figure 6.
Cart velocity.

ISSN: 2576-8484
Vol. 10, No. 9: 290-304, 2026
DOI: 10.55214/2576-8484.v10i9.13602

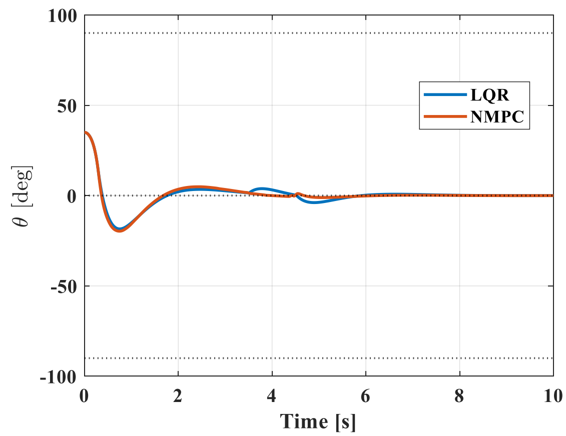

Figure 7.
Rod angular position.

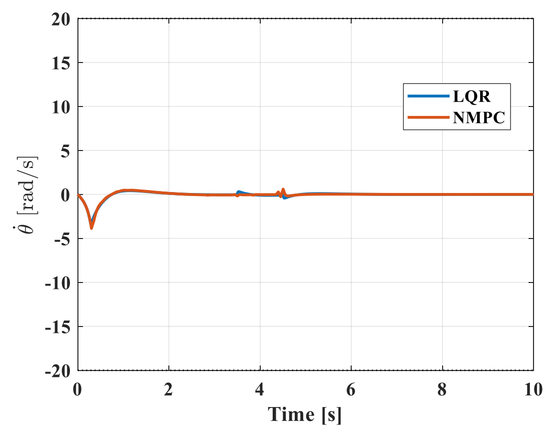

Figure 8.
Rod angular velocity.

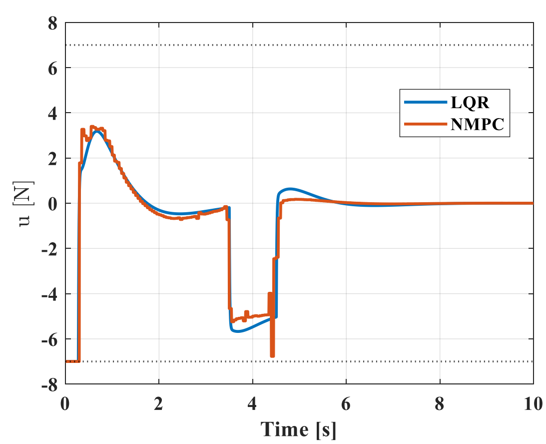

Figure 9.
Control effort.

4.2. Severely Nonlinear Benchmark

ISSN: 2576-8484
Vol. 10, No. 9: 290-304, 2026
DOI: 10.55214/2576-8484.v10i9.13602

A substantial difference in behavior can be observed between the two control strategies. As shown in Figures 10 and 11, the NMPC controller successfully maintains the cart position and velocity within acceptable bounds throughout the simulation. In contrast, the LQR controller loses its ability to stabilize the system after approximately 4.5 s, leading to a rapid divergence of the cart position and velocity. Similar observations can be made in Figures 12 and 13, where the pendulum angle and angular velocity remain bounded under NMPC control, whereas the LQR response exhibits growing oscillations and ultimately becomes unstable. The control inputs depicted in Figure 14 further indicate that the instability is not caused by excessive actuator demand, but rather by the inability of the linearized LQR design to cope with the strong nonlinear dynamics and uncertainty levels encountered in this scenario.

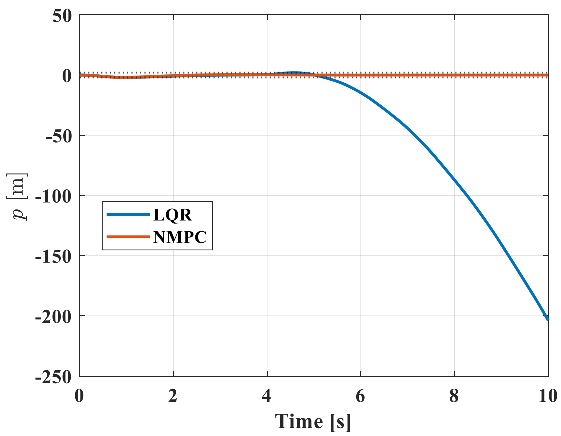

Figure 10.
Cart position.

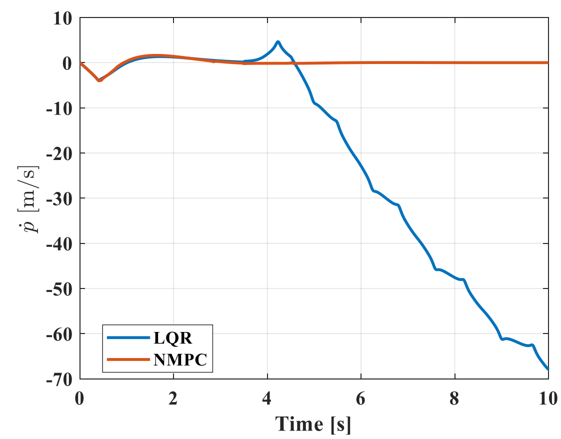

Figure 11.
Cart velocity.

ISSN: 2576-8484
Vol. 10, No. 9: 290-304, 2026
DOI: 10.55214/2576-8484.v10i9.13602

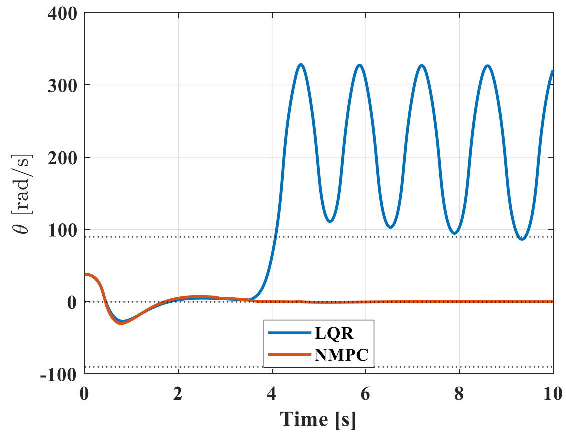

Figure 12.
Rod angular position.

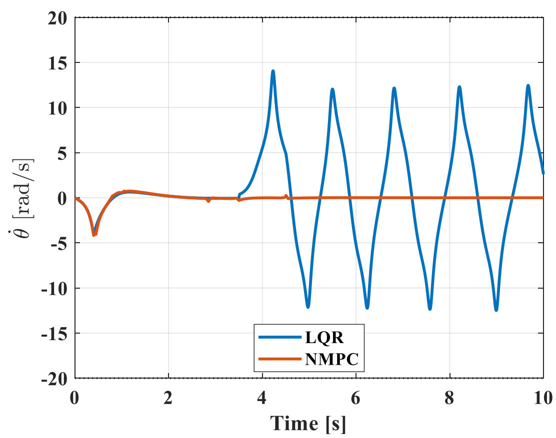

Figure 13.
Rod angular velocity.

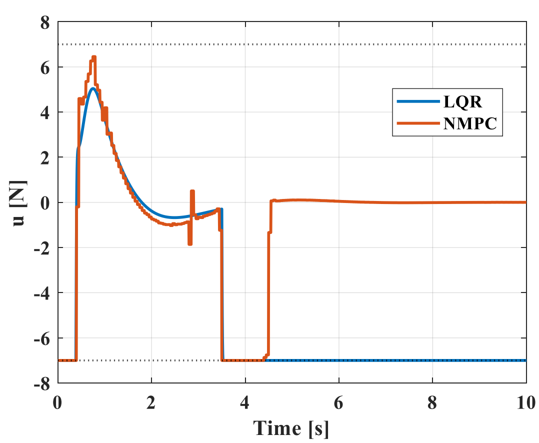

Figure 14.
Control effort.

The quantitative results reported in Table 4 corroborate the visual observations. Relative to LQR, the NMPC controller reduces the RMS pendulum angle by 94.48%, the maximum angular deviation by 88.42%, the RMS cart displacement by 99.15%, and the maximum cart displacement by 99.08%. Moreover, significant reductions are achieved for the control-related performance indices, including 96.62% for IAE_θ and 99.40% for ITAE_θ. Most importantly, the NMPC-controlled system remains stable with a settling time of 4.745 s, whereas the LQR-controlled system becomes unstable; therefore, no meaningful settling time can be defined.

These results clearly demonstrate that the proposed NMPC controller preserves closed-loop stability and maintains satisfactory performance, even when the system operates far from the equilibrium region. Conversely, the LQR controller, which is designed from a local linear approximation, exhibits a limited operating range and fails when confronted with severe nonlinearities, large disturbances, and model uncertainties. Consequently, the advantages of NMPC become particularly evident under demanding operating conditions, where accurate nonlinear prediction and constraint handling are essential.

5. Conclusion

This paper presented a nonlinear model predictive control (NMPC) strategy for stabilizing an inverted pendulum on a cart under disturbances and model uncertainties. The controller was evaluated using moderately and severely nonlinear benchmark scenarios and compared with a conventional linear quadratic regulator (LQR) controller.

Simulation results showed that both controllers achieved satisfactory performance under moderate nonlinear conditions. However, under severe nonlinearities and disturbances, the LQR controller became unstable, whereas the NMPC controller successfully maintained pendulum stabilization and cart-position regulation. These results demonstrate the superior robustness and disturbance-rejection capability of NMPC when the system operates far from equilibrium.

Future work will focus on reducing the computational complexity of the NMPC algorithm while preserving its control performance for faster real-time applications.

Transparency:

The authors confirm that the manuscript is an honest, accurate, and transparent account of the study; that no vital features of the study have been omitted; and that any discrepancies from the study as planned have been explained. This study followed all ethical practices during writing.

References

[1] L. Chrif, M. Mohammed, Z. Kadda, and M. Youssouf, "Model predictive control for nonlinear inverted pendulum mobile robot with disturbance," *International Journal of Communication Networks and Information*, vol. 16, no. 4, pp. 1918 -1928, 2024.

[2] L. Chrif and K. Zemalache Meguenni Kadda, "Aircraft control system using model predictive controller," *TELKOMNIKA Indonesian Journal of Electrical Engineering*, vol. 15, no. 2, pp. 259–269, 2015.

[3] M. Mohammed, Z. M. Kada, O. A. Hafid, and L. Motefai, "Electrical vehicle modeling and backstepping control," *Indonesian Journal of Electrical Engineering and Computer Science*, vol. 1, no. 1, pp. 60-70, 2016.

[4] L. Chrif, M. Mohammed, and Z. Kadda, "MPC dynamic methodology for lateral and longitudinal motion of flight control," *Journal of Electrical Systems*, vol. 20, no. 3, pp. 4557-4567, 2024.

[5] P. T. Jardine, M. Kogan, S. N. Givigi, and S. Yousefi, "Adaptive predictive control of a differential drive robot tuned with reinforcement learning," *International Journal of Adaptive Control and Signal Processing*, vol. 33, no. 2, pp. 410–423, 2019. https://doi.org/10.1002/acs.2882

[6] A. Reda, A. Bouzid, and J. Vásárhelyi, "Model predictive control for automated vehicle steering," *Acta Polytechnica Hungarica*, vol. 17, no. 7, pp. 163-182, 2020.

[7] X. Liu, J. Ou, D. Yan, Y. Zhang, and G. Deng, "Path tracking control of automated vehicles based on adaptive MPC in variable scenarios," *IET Intelligent Transport Systems*, vol. 18, no. 6, pp. 1031-1044, 2024. https://doi.org/10.1049/itr2.12484
[8] S. Bouzoualegh, E.-H. Guechi, and R. Kelaiaia, "Model predictive control of a differential-drive mobile robot," *Acta Universitatis Sapientiae, Electrical and Mechanical Engineering*, vol. 10, no. 1, pp. 20-41, 2018. https://doi.org/10.2478/auseme-2018-0002
[9] M. Mekkaoui and M. K. Zemalache, "Dynamic sliding mode and backstepping controllers for trajectory tracking of mobile robot wheeled," *Przegląd Elektrotechniczny*, vol. 100, no. 4, pp. 221–227, 2024. https://doi.org/10.15199/48.2024.04.43
[10] M. Auzan, R. M. Hujja, M. R. Fuadin, and D. Lelono, "Path tracking and position control of nonholonomic differential drive wheeled mobile robot," *Jurnal Ilmiah Teknik Elektro Komputer dan Informatika*, vol. 7, no. 3, pp. 368-379, 2021. https://doi.org/10.26555/jiteki.v7i3.21017
[11] F. Fahmizal, M. Arrofiq, R. Adrian, and A. Mayub, "Two-wheeled inverted pendulum (TWIP) robot with Linear Quadratic Regulator (LQR) control," *ELKOMIKA: Jurnal Teknik Energi Elektrik, Teknik Telekomunikasi, & Teknik Elektronika*, vol. 7, no. 2, pp. 224–237, 2019. https://doi.org/10.26760/elkomika.v7i2.224
[12] D. Wang, W. Wei, Y. Yeboah, Y. Li, and Y. Gao, "A robust model predictive control strategy for trajectory tracking of omni-directional mobile robots," *Journal of Intelligent & Robotic Systems*, vol. 98, pp. 439-453, 2020. https://doi.org/10.1007/s10846-019-01083-1
[13] A. S. Al-Araji, "An adaptive swing-up sliding mode controller design for a real inverted pendulum system based on Culture-Bees algorithm," *European Journal of Control*, vol. 45, pp. 45-56, 2019. https://doi.org/10.1016/j.ejcon.2018.12.001
[14] A. Ibrar, S. Ahmad, A. Safdar, and N. Haroon, "Efficiency enhancement strategy implementation in hybrid electric vehicles using sliding mode control," *Electrical Engineering & Electromechanics*, no. 1, pp. 10-19, 2023. https://doi.org/10.20998/2074-272X.2023.1.02
[15] J. M. K. Kowalski and S. A. Habib, "Hybrid control of a double linear inverted pendulum using LQR-fuzzy and LQR-PID controllers," presented at the 2022 IEEE International Conference on Mechatronics and Automation (ICMA) (pp. 1784–1789). IEEE, 2020.
[16] M. K. Habib and S. A. Ayankoso, "Hybrid control of a double linear inverted pendulum using LQR-fuzzy and LQR-PID controllers," in *2022 IEEE International Conference on Mechatronics and Automation (ICMA) (pp. 1784-1789). IEEE*, 2022.
[17] L. Chrif, Z. M. Kadda, and L. Mohammed, "LQR controller and optimal estimation observer design applied for pitch aircraft B747," *Indonesian Journal of Systems Signal Control and Engineering Application*, vol. 13, no. 3, pp. 53-58, 2020.
[18] S. Coşkun, "Non-linear control of inverted pendulum," *Çukurova Üniversitesi Mühendislik-Mimarlık Fakültesi Dergisi*, vol. 35, no. 1, pp. 27-38, 2020.
[19] S. Bacha, R. Saadi, M. Y. Ayad, M. Sahraoui, K. Laadjal, and A. J. M. Cardoso, "Autonomous electric-vehicle control using speed planning algorithm and back-stepping approach," *Energies*, vol. 16, no. 5, p. 2459, 2023. https://doi.org/10.3390/en16052459
[20] R. Pete and M. D. Deosarkar, "Automatic braking system," *Journal of Electrical Systems*, vol. 20, no. 7s, pp. 957–964, 2024. https://doi.org/10.52783/jes.3476
[21] S. Wei, P. E. Pfeffer, and J. Edelmann, "State of the art: Ongoing research in assessment methods for lane keeping assistance systems," *IEEE Transactions on Intelligent Vehicles*, vol. 9, no. 9, pp. 5853-5875, 2023. https://doi.org/10.1109/TIV.2023.3269156
[22] H. Liu, C. Liu, L. Hao, and D. Zhang, "Stability analysis of lane-keeping assistance system for trucks under crosswind conditions," *Applied Sciences*, vol. 13, no. 17, p. 9891, 2023. https://doi.org/10.3390/app13179891
[23] J. Ortega, H. Lengyel, and Z. Szalay, "Overtaking maneuver scenario building for autonomous vehicles with PreScan software," *Transportation Engineering*, vol. 2, p. 100029, 2020. https://doi.org/10.1016/j.treng.2020.100029
[24] G. Mandai, D. Bhattacharya, and P. De, "Real time vision based overtaking assistance system for drivers at night on two-lane single carriageway," *Computación y Sistemas*, vol. 25, no. 2, pp. 403-416, 2021. https://doi.org/10.13053/cys-25-2-3783